INSTITUTE OF PHYSICS PUBLISHING SEMICONDUCTOR SCIENCE AND TECHNOLOGY
Semicond. Sci. Technol. **20** (2005) 625–631 doi:10.1088/0268-1242/20/6/025

Temperature dependence of electrical parameters of the Au/n-InP Schottky barrier diodes

Hidayet Cetin[1] **and Enise Ayyildiz**[2]

[1] Department of Physics, Yozgat Faculty of Arts and Sciences, Erciyes University, 66100 Yozgat, Turkey
[2] Department of Physics, Faculty of Arts and Sciences, Erciyes University, 38039 Kayseri, Turkey

E-mail: enise@erciyes.edu.tr

Received 18 October 2004, in final form 30 March 2005
Published 3 May 2005
Online at stacks.iop.org/SST/20/625

Abstract
The temperature dependence of current–voltage (I–V) and capacitance–voltage (C–V) characteristics of the Au/n-InP Schottky barrier diodes has been measured in the temperature range of 80–320 K. The forward I–V characteristics are analysed on the basis of standard thermionic emission (TE) theory and the assumption of a Gaussian distribution of the barrier heights (BHs). It has been shown that the ideality factor decreases while the barrier height increases with increasing temperatures, on the basis of TE theory. Furthermore, the homogeneous BH value of approximately 0.524 eV for the device has been obtained from the linear relationship between the temperature-dependent experimentally effective BHs and ideality factors. The modified Richardson plot, according to inhomogeneity of the BHs, has a good linearity over the temperature range. The value of Richardson constant A^* has been found to be 5.97 A cm^{-2} K^{-2}, which is close to the theoretical value of 9.4 A cm^{-2} K^{-2} for n-InP. Moreover, the temperature coefficient of the BH is found to be -3.16×10^{-4} eV K^{-1} for Au/n-InP.

1. Introduction

Metal–semiconductor (MS) structures are important research tools in the characterization of new semiconductor materials and, at the same time, the fabrication of these structures plays a crucial role in constructing some useful devices in technology [1–4]. Indium phosphide (InP) has been particularly interesting as a substrate for opto-electronic applications and high-speed electronic devices due to a direct transition band gap and high electron mobility, both of which are very important in these devices [4–6]. However, a serious drawback of InP is the low Schottky barrier height (BH). This increases the leakage current, and the device performance is degraded. Schottky barrier diodes (SBDs) with low BH have found applications in devices operating at cryogenic temperatures as infrared detectors and sensors in thermal imaging [7, 8]. The performance and reliability of an SBD are drastically influenced by the interface quality between the deposited metal and the semiconductor surface. Therefore, the formation and characterization of metal/InP devices have been the subject of a vast number of fundamental studies [9–18]. The observed current–voltage (I–V) characteristics of the real SBDs usually deviate from the ideal thermionic emission (TE) model, such as the strong dependence of both BH and the ideality factor on temperature, the difference in BHs obtained from different methods and the nonlinearity of the Richardson plots [19–33].

In the literature, there are many mechanisms to explain these deviations, such as generation–recombination current, contamination in the interface, an intervening insulation layer, deep impurity levels, edge leakage currents, different atomic adsorbents inducing similar disruptions of the semiconductor surface lattice and the effect of image force lowering [1–4]. On the other hand, it has been pointed out that the BH is inhomogeneous in the metal–semiconductor (MS) interface. It may contain patches with low barrier height. The total

current is the sum of the currents through all of these patches and the current through the whole contact area [19–31].

Moreover, if the patch area is small (less than or comparable to the depletion layer), the pinch-off effect will be taken into account, i.e. the effective reduction of the BHs between the patch and the surrounding area is smaller than its original drop in the metal–semiconductor interface [21, 28]. In the literature, currents through both the patches and the whole contact area current are usually assumed to be thermionic emission. The total current has a similar expression as the traditional TE model with an apparent BH and an apparent ideality factor that are temperature dependent.

In this study, the current–voltage (I–V) and capacitance–voltage (C–V) measurements of Au Schottky contacts on an n-InP substrate have been made over the temperature range of 80–320 K. The temperature-dependent barrier characteristics of the Au/n-InP SBDs have been interpreted on the basis of the existence of Gaussian distribution of the BHs around a mean value due to BH inhomogeneities at the MS interface.

2. Experimental procedure

The undoped n-type (1 0 0) InP substrate having a resistivity of 0.26 Ω cm, an electron mobility of 5280 $cm^2\ V^{-1}\ s^{-1}$ and polished on one side has been used. The wafer is chemically cleaned using ultrasonic agitation in trichloroethylene, acetone and methanol for 5 min and then rinsed in de-ionized water of 18 MΩ and dried with high purity N_2. The cleaning procedure is followed by a 60 s dip in HF:H_2O (1:10) solution to remove the native oxide on the front surface of the substrate. The wafer is inserted into the deposition chamber immediately after the etching process. Ohmic contacts are made by evaporation of In on the non-polished side of the InP wafer and then by thermal annealing at 350 °C for 60 s in flowing nitrogen in a quartz tube furnace. The wafer is immediately inserted into the evaporation chamber for forming Schottky contacts. The metal gate, Au, is then deposited through a molybdenum mask by thermal evaporation to form circular dots with a diameter of approximately 1 mm. The exact shape and area of the diode are evaluated by using a stereomicroscope. All evaporation processes are carried out in a turbo-molecular fitted vacuum coating unit at about $2–5 \times 10^{-5}$ Pa.

The current–voltage (I–V) and capacitance–voltage (C–V) measurements have been made automatically using a HP 4140B picoammeter and an HP model 4192 A LF impedance analyser, respectively, in the dark. The diode was cooled by liquid N_2 and the variation of the temperature is better than ±1 K during each temperature point of measurement.

3. Experimental results and discussion

3.1. The current–voltage and capacitance–voltage characteristics of the Schottky barrier diodes as functions of temperature

The semi-logarithmic I–V characteristics of the Au/n-InP (1 0 0) SBDs in the temperature range of 80–320 K in steps of 20 K are shown in figure 1. We analyse the experimental I–V curves according to thermionic emission theory in which the current–voltage characteristics are given by the relation [1–4]

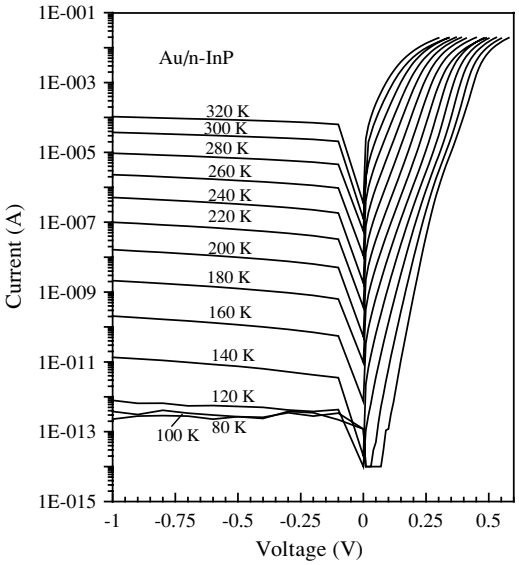

Figure 1. Semi-log reverse and forward current–voltage characteristics of the Au/n-InP Schottky barrier diode at different temperatures.

$$I = I_0 \exp\left(\frac{qV}{nkT}\right)\left[1 - \exp\left(-\frac{qV}{kT}\right)\right], \tag{1}$$

where V is the applied voltage, k is Boltzmann's constant, T is the temperature in kelvins, q is the charge on the electron, the ideality factor n is written as

$$n = \frac{q}{kT}\left(\frac{\mathrm{d}V}{\mathrm{d}(\ln I)}\right) \tag{2}$$

and the saturation current I_0, derived from the straight line intercept of $\ln I$ at $V = 0$, is expressed [1–4] as

$$I_0 = AA^*T^2 \exp\left(-\frac{q\Phi_{b0}}{kT}\right), \tag{3}$$

where A is the diode area, A^* is the effective Richardson constant (taken as 9.4 A $cm^{-2}\ K^{-2}$ for n-type InP) and Φ_{b0} is the apparent BH. The reverse saturation current I_0 decreased sharply with the decrease of the temperature, as can be seen in figure 1. The experimental values of the apparent BH Φ_{b0} and the ideality factor n are determined from intercepts and slopes of the forward bias $\ln I$ versus voltage (V) plot according to TE theory at each temperature, respectively. The values of the apparent BH and ideality factor have been changed from 0.274 eV and 2.321 at 80 K to 0.516 eV and 1.054 at 320 K, respectively. The values for the BH are effective values and do not take into account image force lowering.

Figure 2 shows the values of n (represented by open diamonds) obtained from the linear portion of the forward bias current–voltage characteristics in figure 1. As can be seen in figure 2, the experimental values of n increased with a decrease in temperature.

The experimental reverse bias C^{-2}–V characteristics of the Au/n-InP (1 0 0) SBD in the temperature range of 80–320 K in steps of 20 K are shown in figure 3. The dependence on the temperature of Φ_{bn} (IV) (filled diamonds) and Φ_{bn} (CV) (open diamonds) obtained, respectively, from the forward bias I–V and reverse bias C^{-2}–V characteristics, is given in figure 4. The experimental value of Φ_{bn} (IV) decreased with a decrease

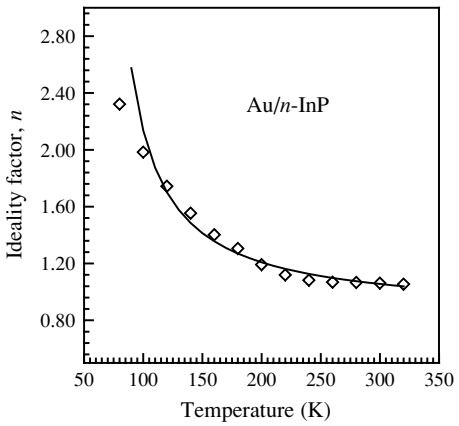

Figure 2. Temperature dependence of the ideality factor for the Au/n-InP Schottky barrier diode in the temperature range of 80–320 K. The continuous curve represents the estimated value of ideality factor using equation (12) with $\rho_2 = 0.187$ V and $\rho_3 = 0.0124$ V.

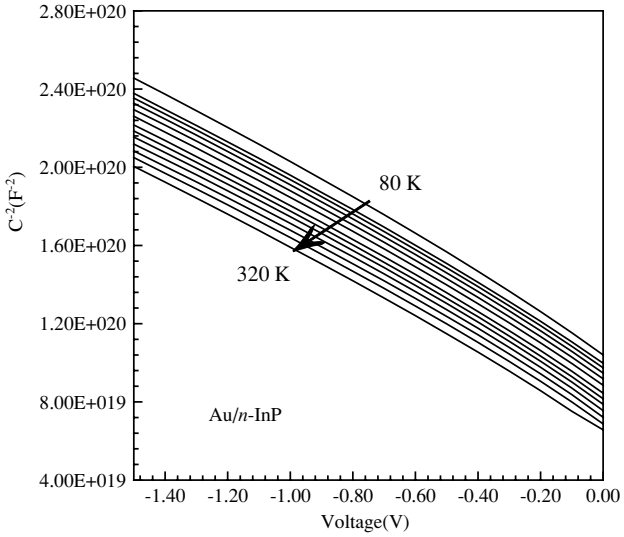

Figure 3. The reverse bias C^{-2}–V characteristics of the Au/n-InP Schottky barrier diode at different temperatures.

in the temperature. As explained in [20, 21], since current transport across the MS interface is a temperature-activated process, at low temperature, electrons are able to surmount the lower barriers, and therefore current transport will be dominated by current flowing through the patches of lower BH and a larger ideality factor. As the temperature increases, more and more electrons have sufficient energy to surmount the higher barriers. As a result, both $\Phi_b\,(IV)$ and n are strongly dependent on temperature.

Due to the square dependence of $\Phi_{bn}(CV)$ on $1/C$, compared to the logarithmic dependence of $\Phi_{bn}(IV)$ on the current, $\Phi_{bn}(CV)$ is more sensitive to the experimental error of the measurement data than $\Phi_{bn}(IV)$, as pointed out by Zhu *et al* [29]. Moreover, it is clearly seen from figure 4 that the barrier height $\Phi_{bn}(CV)$ obtained from the C^{-2}–V characteristics increases with decreasing temperature. Then, the temperature dependence of the $\Phi_{bn}(CV)$ is expressed as

$$\Phi_{bn}\,(CV) = \Phi_{bn}\,(T = 0) + \alpha T, \tag{4}$$

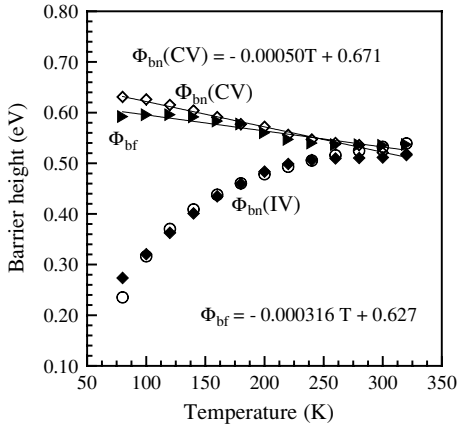

Figure 4. Temperature dependence of the zero-bias apparent barrier height, flat-band barrier height and C–V barrier height for the Au/n-InP Schottky barrier diode. The open circles represent the estimated value of Φ_{ap} using equation (11) with $\bar{\Phi}_{b0}\,(T = 0) = 0.640$ eV and $\sigma_0 = 0.0748$ V.

where $\Phi_{bn}\,(T = 0)$ is the barrier height extrapolated to zero temperature and α is the temperature coefficient of the barrier height. The fit of equation (4) to the data shown in figure 4 gives $\alpha = -5 \times 10^{-4}$ eV K^{-1} which is the temperature coefficient of the InP band gap [15] and $\Phi_{bn}(T = 0) = 0.672$ eV.

In order to obtain the flat-band barrier height, the analyses of Wagner *et al* [34] and Chin *et al* [35] have been followed. The flat-band barrier height is given by [34, 35]

$$\Phi_{bf} = n\Phi_{b0}\,(IV) - (n-1)\,\frac{kT}{q}\ln\left(\frac{N_c}{N_d}\right), \tag{5}$$

where N_c and N_d are, respectively, the effective density of states in the conduction band and the donor density. N_c is defined as $2(2m^*kT/h^2)^{3/2}$ with m^* being the majority carrier effective mass, $m^* = 0.077\ m_e$ for n-InP [4, 36]. The experimental carrier concentrations depending on the temperature are calculated from the reverse bias C^{-2}–V characteristics in figure 3. The temperature-dependent N_c and N_d values are used in calculating Φ_{bf} values. The values of N_d and N_c are 2.139×10^{15} cm^{-3} and 1.052×10^{17} cm^{-3} at 80 K and 2.14×10^{15} cm^{-3} and 6.020×10^{17} cm^{-3} at 320 K, respectively. The flat-band barrier height of the Au/n-InP SBDs is calculated from I–V barrier heights and the corresponding ideality factor at each temperature. Figure 4 shows variation of the flat-band barrier height Φ_{bf} (represented by filled triangles) as a function of the temperature. As can be seen, the flat-band barrier height is invariably larger than the zero-bias barrier height at low temperature. In fact, the flat-band barrier height mirrors $\Phi_{bn}(CV)$ but with slightly different values of the parameters in equation (5) of $\Phi_{bf}(T = 0) = 0.630$ eV and $\alpha = -3.16 \times 10^{-4}$ eV K^{-1}. This is possibly due to extremely high values of the ideality factor, which increases with decreasing temperature. In contrast to the case of the zero-bias BH, the electric field in the semiconductor is zero under the flat-band conditions and thus the semiconductor bands are flat, which eliminates the effect of tunnelling and image force lowering that would affect the I–V characteristics and removes the influence of lateral inhomogeneity.

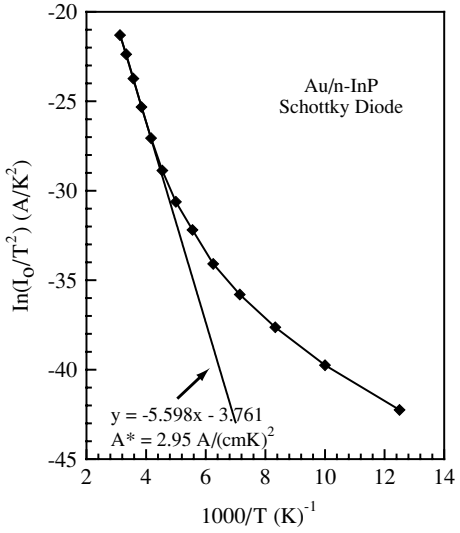

Figure 5. Richardson plot of $\ln(I_0/T^2)$ versus $10^3/T$ for the Au/n-InP Schottky barrier diode.

The Richardson plot is drawn to obtain the barrier height in another way. From equation (3), we can rewrite

$$\ln\left(\frac{I_0}{T^2}\right) = \ln(AA^*) - \frac{q\Phi_{b0}}{kT}. \tag{6}$$

The saturation current I_0 is found from the intercept of the straight lines in figure 1 with the ordinate. Figure 5 shows the $\ln(I_0/T^2)$ versus $1000/T$ curve. According to equation (6), the plot $\ln(I_0/T^2)$ versus $1/T$ yields a straight line with a slope given by the barrier height at 0 K, and the intercept given by the Richardson constant. The bowing of the curve in figure 5 demonstrates that it is impossible to fit our data in the whole temperature range. The experimental data are seen to fit asymptotically to a straight line at higher temperature only. However, for $T > 240$ K, the experimental points lie on a straight line. The value of A^* obtained from the intercept of the straight portion at the ordinate is equal to 2.95 A cm^{-2} K^{-2}, which is lower than the known value of 9.4 A cm^{-2} K^{-2}. A BH value of 0.48 eV from the slope of this straight line is obtained for the device. The bowing of the experimental $\ln(I_0/T^2)$ versus $1/T$ plot is caused by the temperature dependence of the BH. As will be discussed below, the deviation in the Richardson plots may be due to the spatially inhomogeneous barrier heights and potential fluctuations at the interface that consist of low and high barrier areas [19–25], that is, the current through the diode will flow preferentially through the lower barrier in the potential distribution [19–25].

3.2. The effect of inhomogeneous barrier height

The ideality factor is simply a manifestation of the barrier uniformity and it increases for an inhomogeneous barrier [23]. An apparent increase in ideality factor and decrease in BH at low temperature are possibly caused by some other effects such as inhomogeneities of thickness and composition of the layer, non-uniformity of the interfacial charges or the presence of a thin insulating layer between the metal and the semiconductor [19–25]. Since current transport across the MS interface is a temperature-activated process, at low temperature, the current

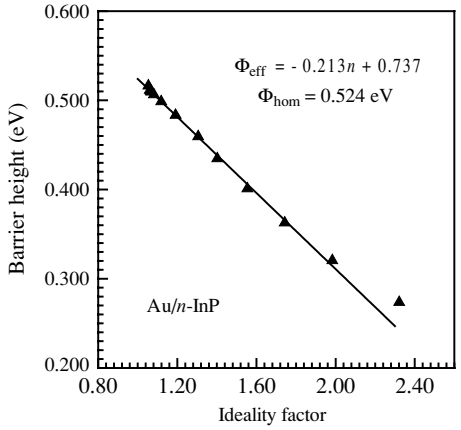

Figure 6. The zero-bias apparent barrier height versus ideality factor with temperature for the Au/n-InP Schottky barrier diode.

will be dominated by the current through the patches of low BH. Moreover, simulation studies of Freeouf *et al* [37] on mixed-phase Schottky contact reveal that, below a critical size, low BH region pinched off and only high barrier remains effective. Similar results obtained for the PtSi/Si diodes have been explained with an analytical potential fluctuation model for the interpretation of current–voltage and capacitance–voltage measurements on spatially inhomogeneous Schottky contacts proposed by Werner and Güttler [20]. According to Henisch [2], fluctuations in barrier heights are unavoidable, as they exist even in the most carefully fabricated systems.

Schmitsdorf *et al* [38] used Tung's theoretical approach and they found a linear correlation between the experimental zero-bias BH and the ideality factors n. Figure 6 shows a plot of the experimental SBH as a function of the ideality factors dependent on temperature. As can be seen from figure 6, there is a linear relationship between the experimentally effective BHs and the ideality factors of the Au/n-InP SBDs that is explained by lateral inhomogeneities of the BHs in the SBDs [38]. The extrapolation of the experimental SBHs versus ideality factors plot to $n = 1$ has given a homogeneous BH of approximately 0.524 eV. The other barrier height values deviate from this value due to local inhomogeneities. The homogeneous BH value of 0.524 eV is in agreement with 0.500 eV obtained by Brillson *et al* [16], Anand *et al* [17] and Hökelek and Robinson [18] on the Au/n-type InP Schottky barrier diodes.

In order to describe the above abnormal behaviours, it can be used as an analytical potential fluctuation model on spatially inhomogeneous Schottky barrier diodes [19–25, 27–31]. The different types of barrier distribution function at the interface have been reported [20]. Let us assume that the distribution of the BHs is a Gaussian distribution of the BHs with a mean value $\bar{\Phi}_b$ and a standard deviation σ [19–25] in the form

$$P(\Phi_b) = \frac{1}{\sigma\sqrt{2\pi}} \exp\left[-\left(\frac{\Phi_b - \bar{\Phi}_b}{2\sigma^2}\right)^2\right], \tag{7}$$

where the pre-exponential term is the normalization constant. Then, the total current across the Schottky barrier diode at a forward bias is given by

$$I(V) = \int_{-\infty}^{\infty} I(\Phi_b, V)\, P(\Phi_b)\, d\Phi, \tag{8}$$

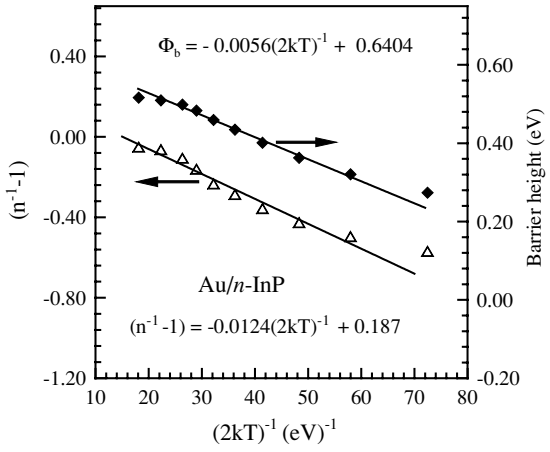

Figure 7. The zero-bias apparent barrier height and ideality factor versus $1/2kT$ curves of the Au/n-InP Schottky barrier diode according to Gaussian distribution of BHs.

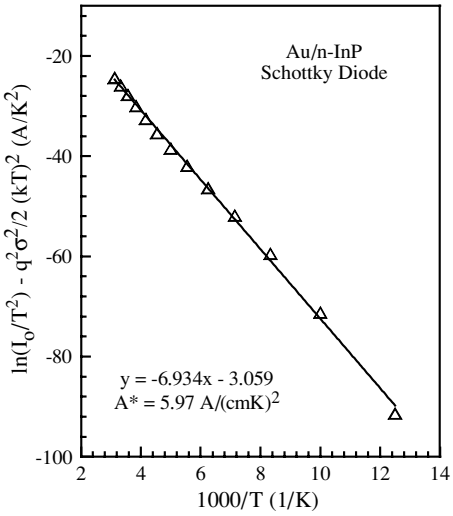

Figure 8. The modified Richardson $\ln(I_0/T^2) - q^2\sigma_0^2/2(kT)^2$ versus $10^3/T$ plot for the Au/n-InP Schottky barrier diode according to Gaussian distribution of BHs.

where $I(\Phi_b, V)$ is the current at a bias V for a barrier of Φ_b based on the thermionic emission model. It is assumed that the mean BH $\bar{\Phi}_b$ and σ are linearly bias dependent on Gaussian parameters, such as $\bar{\Phi}_b = \bar{\Phi}_{b0} + \rho_2 V$ and standard deviation $\sigma = \sigma_0 + \rho_3 V$, where ρ_2 and ρ_3 are voltage coefficients which may depend on T. The temperature dependence of σ is usually small and may be neglected [19, 20]. Substituting equations (1) and (7) into equation (8), and performing the integration it becomes [19, 20]

$$I(V) = I_0 \exp\left(\frac{qV}{kTn_{ap}}\right)\left[1 - \exp\left(-\frac{qV}{kT}\right)\right], \qquad (9)$$

with

$$I_0 = AA^*T^2 \exp\left(-\frac{q\Phi_{ap}}{kT}\right), \qquad (10)$$

where Φ_{ap} and n_{ap} are the apparent BH and apparent ideality factor, respectively, and are given by

$$\Phi_{ap} = \bar{\Phi}_{b0} - \frac{q\sigma_0^2}{2kT}, \qquad (11)$$

$$\left(\frac{1}{n_{ap}} - 1\right) = \rho_2 - \frac{q\rho_3}{2kT}. \qquad (12)$$

Fitting of the experimental data into equations (3) or (10) and in equation (2) yields Φ_{ap} and n_{ap}, respectively, which obey equations (11) and (12). Thus, the plot of Φ_{ap} versus $1/2kT$ (figure 7) must be a straight line that yields $\bar{\Phi}_{b0}$ and σ_0 from the intercept and slope, respectively. The values of 0.640 eV and 0.0748 eV for $\bar{\Phi}_{b0}$ and σ_0, respectively, are deduced from the experimental Φ_{ap} versus $1/2kT$ plot. Moreover, as can be seen in figure 4, the experimental results of Φ_{ap} fit very well with theoretical equation (11) with $\bar{\Phi}_{b0}$= 0.640 eV and σ_0= 0.0748 eV. The open circles in figure 4 represent data estimated with these parameters using equation (11). Thus, the standard deviation is ∼11.7% of the mean barrier height. The standard deviation is a measure of the barrier homogeneity. The lower value of σ_0 corresponds to more homogeneous BH. It is clear that the diode with the best rectifying performance presents the best barrier homogeneity with the lower value of standard deviation.

Furthermore, Calvet *et al* [39] have shown experimentally that the barrier inhomogeneities become less important in devices with smaller contact areas. It is seen that the value of $\sigma_0 = 0.0748$ eV is not small compared to the mean value of $\bar{\Phi}_{bo} = 0.640$ eV, and it indicates the presence of the interface inhomogeneities and thus potential fluctuation.

Figure 7 shows the plot of n_{ap} versus $1/2kT$ having a straight line yields voltage coefficients ρ_2 and ρ_3 from the intercept and slope, respectively. The values of $\rho_2 = -0.187$ V and $\rho_3 = -0.0124$ V are deduced from the experimental n_{ap} versus $1/2kT$ plot. The linear behaviour of this plot reveals that the ideality factor does indeed express the voltage deformation of the Gaussian distribution of the BH. Furthermore, the experimental results of n_{ap} fit very well with theoretical equation (12) with $\rho_2 = -0.187$ V and $\rho_3 = -0.0124$ V. The continuous solid line in figure 2 indicates data estimated with these parameters using equation (12). Combining equations (10) and (11), the conventional Richardson plot is modified:

$$\ln\left(\frac{I_0}{T^2}\right) - \left(\frac{q^2\sigma_0^2}{2k^2T^2}\right) = \ln(AA^*) - \frac{q\bar{\Phi}_{b0}}{kT}. \qquad (13)$$

A modified $\ln(I_0/T^2) - q^2\sigma_0^2/2(kT)^2$ versus $1000/T$ plot according to equation (9) must give a straight line with the slope directly yielding the mean $\bar{\Phi}_{b0}$ and the intercept (= $\ln(AA^*)$) at the ordinate determining A^* for a given diode area A. Figure 8 represents this plot. The modified $\ln(I_0/T^2) - q^2\sigma_0^2/2(kT)^2$ versus $1000/T$ plots yields $\bar{\Phi}_{b0}$ and A^* as 0.600 eV and 5.94 A cm^{-2} K^{-2}, respectively, without using the temperature coefficient of the BH. As is seen, the value of $\bar{\Phi}_{b0} = 0.600$ eV from this plot is in close agreement with the value of $\bar{\Phi}_{b0} = 0.640$ eV from the plot of n_{ap} versus $1/2kT$ (figure 7).

The difference between $\Phi_{bn}(IV)$ and $\Phi_{bn}(CV)$, as well as the strong temperature dependence of $\Phi_{bn}(IV)$ and n at low temperature, can also be explained by assuming a Gaussian distribution of BHs with a mean value Φ_{bn} and a standard deviation σ [19–25]. The capacitance depends only on the mean band bending and is insensitive to the standard deviation σ of the barrier height distribution [20]. Assuming a Gaussian

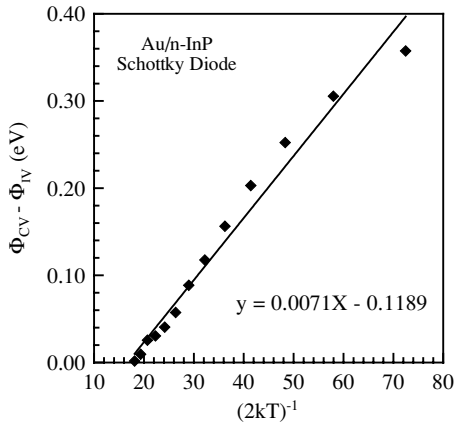

Figure 9. The experimental $\Phi_{bn}(CV) - \Phi_{bn}(IV)$ versus $1/2kT$ curves of the Au/n-InP Schottky barrier diode according to Gaussian distribution of BHs.

distribution of the BH with mean value $\bar{\Phi}_b$ and a standard deviation of the BH σ_0 at zero bias according to [20], it is seen that the apparent BH from the experimental forward bias *I–V* plot is also related to the mean BH $\bar{\Phi}_b = \bar{\Phi}_b(CV)$ from the experimental reverse bias C^{-2}–*V* plot. The relationship between Φ_{ap} and $\Phi_{bn}(CV)$ is given by

$$\bar{\Phi}_b - \Phi_{ap} = -\frac{q\sigma_0^2}{2kT} + \frac{q\alpha_\sigma}{2k} \tag{14}$$

where α_σ is attributed to the temperature dependence of σ_0. Figure 9 shows the experimental $\Phi_{bn}(IV) - \Phi_{bn}(CV)$ versus $1/2kT$ plot according to equation (14). The plot must give a straight line of slope $\sigma_0^2/2k$ and an ordinate intercept $\alpha_\sigma/2k$ from which the parameters σ_0 and α_σ are determined. The slope and ordinate intercept of the plot gave the values of $\sigma_0 =$ 0.0843 V and $\alpha_\sigma = 2.049 \times 10^{-5}$ V^2 K^{-1}, respectively. This value of σ_0 is in close agreement with the value of $\sigma = 0.0748$ V from the plot of Φ_{ap} versus $1/2kT$ drawn according to equation (11). Therefore, the spatial inhomogeneity of the Schottky barrier heights is not neglected in the analysis of electrical measurements.

4. Conclusion

The *I–V* and *C–V* measurements of the Au/n-InP (1 0 0) SBDs have been made in the temperature range of 80–320 K. The *I–V* characteristics of the Au/n-InP (1 0 0) SBDs taking into account thermionic emission theory for a moderated doped semiconductor have been investigated. The obtained *I–V* BHs are in the range of 0.274–0.516 eV with ideality factor of 2.321–1.054. The ideality factor and the BHs determined from the forward *I–V* characteristics are found to be strong functions of temperature. The origin and the nature of the increase in the ideality factor and decrease in the barrier height with decreasing temperature in the Au/n-InP Schottky barrier diodes have been successfully explained on the basis of the thermionic emission with Gaussian distribution of the barrier heights. This behaviour is attributed to spatial variations of the BHs. The laterally homogeneous SBH value of approximately 0.524 eV for the Au/n-InP (1 0 0) SBDs has been deduced from the linear relationship between the experimental BHs and ideality factors. The values of the flat-band BH are obtained from the temperature dependence of the *I–V* characteristics. The experimental results of Φ_{ap} and n_{ap} fit very well with the theoretical equations related to the Gaussian distribution of Φ_{ap} and n_{ap}. Moreover, the Richardson constant value of 5.97 A cm^{-2} K^{-2} for n-InP is obtained by means of the modified Richardson plot, considering Gaussian distribution of the barrier height.

Acknowledgments

This work has been supported by the Scientific Research Projects Unit of Erciyes University through project no. 02–012–11 EÜBAP. One of us (EA) wishes to record her thanks for the facilities afforded at the Hungarian Academy of Sciences, Research Institute for Technical Physics and Materials Science, in which the electrical measurements have been carried out. The English text has been kindly checked by Dr A. Serdar Öztürk from English Language and Literature Department, Erciyes University.

References

[1] Rhoderick E H and Williams R H 1988 *Metal–Semiconductor Contacts* 2nd edn (Oxford: Clarendon)
[2] Henisch H K 1984 *Semiconductor Contacts* (London: Oxford University) p123
[3] Tung R T 2001 *Mater. Sci. Eng. R.* **35** 1
[4] Wilmsen C W 1985 *Physics and Chemistry of III–V Compound Semiconductor Interfaces* (New York: Plenum)
[5] Hattori K and Torii Y 1991 *Solid-State Electron.* **34** 527
[6] Victorovitch P, Louis P, Besland M P and Chovet A 1995 *Solid-State Electron.* **38** 1035
[7] McCafferty P G, Sellai A, Dawson P and Elabd H 1996 *Solid-State Electron.* **39** 583
[8] Chand S and Kumar J 1996 *Appl. Phys. A* **A63** 171
[9] Akkal B, Benamara Z, Bideux L and Gruzza B 1999 *Semicond. Sci. Technol.* **14** 266
[10] Barret C and Maaref H 1993 *Solid-State Electron.* **36** 879
[11] Ahaitouf A, Losson E and Bath A 2000 *Solid-State Electron.* **44** 515
[12] Shi Z and Anderson W A 1992 *J. Appl. Phys.* **72** 3803
[13] Eftekhari G, Tuck B and de Cogan D 1983 *J. Phys. D: Appl. Phys.* **16** 1099
[14] Quennoughhi Z, Boulkroun K, Remy M, Hugon R and Cussenot J R 1994 *J. Phys. D: Appl. Phys.* **27** 1014
[15] Tsay Y S, Gong B and Mitra S S 1972 *Phys. Rev.* B **6** 2330
[16] Brillson L J, Brucker C F, Katnani A D, Stoffel N G and Margaritondo G 1981 *Appl. Phys. Lett.* **38** 784
[17] Anand S, Carlsson S B, Deppert K, Montelius L and Samuelson L 1996 *J. Vac. Sci. Technol.* B **14** 2794
[18] Hökelek E and Robinson G Y 1983 *J. Appl. Phys.* **54** 5199
[19] Song Y P, Van Meirhaeghe R L, Laflere W H and Cardon F 1986 *Solid-State Electron.* **29** 633
[20] Werner J H and Güttler H H 1991 *J. Appl. Phys.* **69** 1522
Werner J H and Güttler H H 1993 *J. Appl. Phys.* **73** 1315
[21] Sullivan J P, Tung R T, Pinto M R and Graham W R J 1991 *Appl. Phys.* **70** 7403
[22] Chen Y G, Ogura M and Okushi H 2003 *Appl. Phys. Lett.* **82** 4367
[23] Zhu S, Van Meirhaeghe R L, Forment S, Ru G P, Qu X P and Li B Z 2004 *Solid-State Electron.* **48** 1205
[24] Karatas S, Altindal S, Turut A and Ozmen A 2003 *Appl. Surf. Sci.* **217** 250
[25] Gumus A, Turut A and Yalcin N 2002 *J. Appl. Phys.* **91** 245
[26] Horvath Zs J 1996 *Solid-State Electron.* **39** 176
[27] Anilturk O S and Turan R 2000 *Solid-State Electron.* **44** 41

[28] Dobrocka E and Osvald J 1994 *Appl. Phys. Lett.* **65** 575
[29] Zhu S, Van Meirhaeghe R L, Detavernier C, Cardon F, Ru G P, Qu X P and Li B Z 2000 *Solid-State Electron.* **44** 663
[30] Jones F E, Wood B P, Myers J A, Hafer C D and Lonergan M C 1999 *J. Appl. Phys.* **86** 6431
[31] Bandyopadhyay S, Bhattacharyya A and Sen S K 1999 *J. Appl. Phys.* **85** 3671
[32] Horvath Zs J 1992 *Proc. SPIE* **1783** 453
[33] Horváth Zs J, Rakovics V, Szentpáli B and Püspöki S 2003 *Phys. Status Solidi* C **3** 916
[34] Wagner L F, Young R W and Sugarman A 1983 *IEEE Electron Device Lett.* **4** 320
[35] Chin V W L, Green M A and Storey J W V 1990 *Solid-State Electron.* **33** 299
[36] Neamen D A 1992 *Semiconductor Physics and Devices* (Boston: Irwin) p 111
[37] Freeouf J L, Jackson T N, Laux S E and Woodall J M 1982 *Appl. Phys. Lett.* **40** 634
Freeouf J L, Jackson T N, Laux S E and Woodall J M 1982 *J. Vac. Sci. Technol.* **21** 570
[38] Schmitsdorf R F, Kampen T U and Mönch W 1997 *Surf. Sci.* **324** 249
[39] Calvet L E, Wheeler R G and Reed M A 2002 *Appl. Phys. Lett.* **80** 1761